International Journal of Chronic Obstructive Pulmonary Disease Dovepress

Open Access Full Text Article ORIGINAL RESEARCH

A CT-Based Lung Radiomics Nomogram for Classifying the Severity of Chronic Obstructive Pulmonary Disease

Taohu Zhou[1,2,*], Xiuxiu Zhou[1,*], Jiong Ni[3], Yu Guan[1], Xin'ang Jiang[1], Xiaoqing Lin[1,4], Jie Li[1,4], Yi Xia[1], Xiang Wang[1], Yun Wang[1], Wenjun Huang[5], Wenting Tu[1], Peng Dong[2], Zhaobin Li[6], Shiyuan Liu[1], Li Fan[1]

[1]Department of Radiology, Second Affiliated Hospital of Naval Medical University, Shanghai, People's Republic of China; [2]School of Medical Imaging, Shandong Second Medical University, Weifang, Shandong, People's Republic of China; [3]Department of Radiology, Tongji Hospital, School of Medicine, Tongji University, Shanghai, People's Republic of China; [4]College of Health Sciences and Engineering, University of Shanghai for Science and Technology, Shanghai, 200093, People's Republic of China; [5]Department of Radiology, The Second People's Hospital of Deyang, Deyang, Sichuan, People's Republic of China; [6]Department of Radiation Oncology, Shanghai Jiao Tong University Affiliated Sixth People's Hospital, Shanghai, 200233, People's Republic of China

*These authors contributed equally to this work

Correspondence: Li Fan, Department of Radiology, Second Affiliated Hospital of Naval Medical University, No. 415 Fengyang Road, Shanghai, 200003, People's Republic of China, Tel +86 21 81886011, Fax +86 2163587668, Email fanli0930@163.com

Background: Chronic obstructive pulmonary disease (COPD) is a major global health concern, and while traditional pulmonary function tests are effective, recent radiomics advancements offer enhanced evaluation by providing detailed insights into the heterogeneous lung changes.

Purpose: To develop and validate a radiomics nomogram based on clinical and whole-lung computed tomography (CT) radiomics features to stratify COPD severity.

Patients and Methods: One thousand ninety-nine patients with COPD (including 308, 132, and 659 in the training, internal and external validation sets, respectively), confirmed by pulmonary function test, were enrolled from two institutions. The whole-lung radiomics features were obtained after a fully automated segmentation. Thereafter, a clinical model, radiomics signature, and radiomics nomogram incorporating radiomics signature as well as independent clinical factors were constructed and validated. Additionally, receiver-operating characteristic (ROC) curve, area under the ROC curve (AUC), decision curve analysis (DCA), and the DeLong test were used for performance assessment and comparison.

Results: In comparison with clinical model, both radiomics signature and radiomics nomogram outperformed better on COPD severity (GOLD I–II and GOLD III–IV) in three sets. The AUC of radiomics nomogram integrating age, height and Radscore, was 0.865 (95% CI, 0.818–0.913), 0.851 (95% CI, 0.778–0.923), and 0.781 (95% CI, 0.740–0.823) in three sets, which was the highest among three models (0.857; 0.850; 0.774, respectively) but not significantly different ($P > 0.05$). Decision curve analysis demonstrated the superiority of the radiomics nomogram in terms of clinical usefulness.

Conclusion: The present work constructed and verified the novel, diagnostic radiomics nomogram for identifying the severity of COPD, showing the added value of chest CT to evaluate not only the pulmonary structure but also the lung function status.

Keywords: chronic obstructive pulmonary disease, radiomics, computed tomography

Introduction

Chronic obstructive pulmonary disease (COPD) is a common and prevalent respiratory disorder, which also ranks the top 3 leading cause of global mortality. According to the latest epidemiological data, COPD was diagnosed in approximately 300 million people (4% of the global population) in 2021, resulting in 3.2 million deaths annually.[1] The gold standard for diagnosing and evaluating COPD is the pulmonary function test (PFT),[2] which yields the forced expiratory volume in

Received: 16 August 2024
Accepted: 2 December 2024
Published: 11 December 2024

1 second per forced vital capacity (FEV1/FVC) and FEV1 percentage of predicted (FEV1% predicted). According to FEV1% predicted, COPD severity was classified into mild, moderate, severe and very severe.

The epidemiological characteristics of COPD severity is varied in each severity classification. A research in UK indicated that the distribution of COPD patients among different severities was 26.8% for GOLD I, 50.3% for GOLD II, 19.2% for GOLD III and 3.8% for GOLD IV.[3] The same trends are also found in another research (GOLD I: 40.1%; GOLD II: 51.3%; GOLD III: 7.7% and GOLD IV: 0.9%).[4] The severity of COPD is related to the exacerbation risk, mortality and complications. Increasing severity of COPD would result in increased frequency of exacerbation,[5] a major contributor to the mortality. John et al demonstrated that patients with mild COPD had a mean of 0.82 exacerbation per year, and the rates increased to 1.17, 1.61, and 2.01 in patients with moderate, severe, and very severe disease, respectively.[6] Moreover, COPD presents with systemic manifestations or comorbidities, including cardiovascular disease, lung cancer, and sarcopenia. These pulmonary or extrapulmonary manifestations can induce dyspnea, functional decline, reduced exercise capacity, decreased quality of life, and increased mortality.[7,8] Previous study has revealed significantly higher complication rates in severe/extremely severe COPD patients with non-small cell lung cancer (NSCLC) when compared to the mild-to-moderate COPD patients with NSCLC.[9] In addition, the treatment varies with the severity of COPD.[10] Therefore, evaluating the severity of COPD is of great significance.

COPD is characterized by the heterogeneity of the whole-lung. However, PFTs reflect the global condition,[11,12] and it cannot reflect the regional change of the lung tissue. Moreover, PFT requires the patients' cooperation to a large extent and may be inconvenient. Especially during the severe respiratory distress syndrome caused by COVID-19, PFT is more challenging. Imaging plays a great role in the focal structure and functional changes of COPD. It has been reported that different severity of COPD has the different CT morphological features. CT findings of COPD include large airway inflammation, emphysema, and non-emphysematous obstruction caused by small airway disease.[13] Moreover, the presence of worse emphysema, airway wall thickening, and/or bronchiectasis observed on chest CT images are associated with COPD development.[14] Except for the visual and qualitative analyses, some studies have used quantitative imaging for assessing COPD severity and achieved promising results. Cho et al[15] demonstrated that quantitative pulmonary vascular features turned out to be associated with COPD severity and emphysema extent. Estrella et al[16] reported an automatic quantification algorithm to assess the association of tracheal shape with COPD severity. Although, quantitative computed tomography (QCT) has various potential applications in the clinical setting, most studies focus on only one or two aspects of the lung density, airways, and pulmonary vessels. As we know, COPD is a highly heterogeneous disease, the comprehensive evaluation from all the aspects of pathological changes including lung density, airways and pulmonary vessels, is very important.

Significant progress has been achieved in applying artificial intelligence in chest diseases.[17] Radiomics has emerged as a technology that extracts high-throughput information from quantitative imaging features and correlates these factors with clinical information in different disorders.[18–20] In general, radiomics features should be extracted from the region of interest (ROI) of the chest CT images. However, the diffuse and heterogeneous characteristics of COPD makes it difficult to determine a focal and representative ROI. Some studies on COPD severity mainly focus on focal ROIs or model-interpretation methods.[18,21] Our team has found that whole-lung radiomics can differentiate the malignant lung nodules from benign ones, and the lung cancer radiomics derived from the one-stop chest CT can evaluate the lung function status.[22,23] Therefore, we hypothesize that the whole-lung radiomics features derived from chest CT could identify the severity of COPD. If CT-based whole-lung radiomics can identify COPD severity in a routine clinical setting, it would add the value of chest CT, especially for patients difficult to perform the PFT, not only providing the morphological information but also the lung function status. In order to make it easy to use in clinical settings, the present study focused on developing and validating a radiomics nomogram to identify COPD severity in a two-center COPD cohort.

Materials and Methods

Patients

This multicenter study included patients with COPD from two centers, and the study protocols were approved by the ethics committee of the respective institutional centers and registered on clinical trial (ChiCTR2300069929). Due to the

retrospective nature, the informed consent was waived. Full inclusion and exclusion criteria are detailed in the Supplementary material 1. A total of 1099 patients with COPD who underwent PFT between September 2015 and April 2023 were retrospectively collected in the CSD-COPD cohort. The Global Initiative for Chronic Obstructive Lung Disease (GOLD) guidelines were first published in 2001 and have been updated annually. The diagnosis and severity of COPD was based on clinical history and spirometry criteria according to the GOLD guidelines. COPD was regarded as the ratio of post-bronchodilator FEV1 to FVC < 0.7. In this study, the severity of COPD was divided into two stages, namely, mild-moderate airflow obstruction (GOLD grade I–II, FEV1 ≥ 50% of predicted) and severe/very severe airflow obstruction (GOLD grade III–IV, FEV1 < 50% of predicted) according to GOLD criteria.[2] Demographic, including age, gender, height, weight, BMI, smoking status and pack-year smoking history, were derived from medical records. However, pack-year smoking history was not available for the majority of patients (greater than 50% missing values) and therefore could not be analyzed. For model training and verification, patients from Center 1 were randomly divided into the training and internal validation sets in a ratio of 7:3. Figure 1 displays the subject screening process according to the eligibility criteria.

CT Image Acquisition and Pulmonary Function Test

The participants underwent non-contrast chest CT with one of the following scanners, Siemens Force, Philips Brilliance 64 (Philips Healthcare), Philips Brilliance 256 (Philips Healthcare) or United Imaging uCT760 (United Imaging Healthcare) scanner. Image smoothing was applied to decrease the number of mis-registrations of noisy images, ie removing high-frequency noise and ensuring the result reliability. CT machine parameters are detailed in Supplementary material 2. PFT

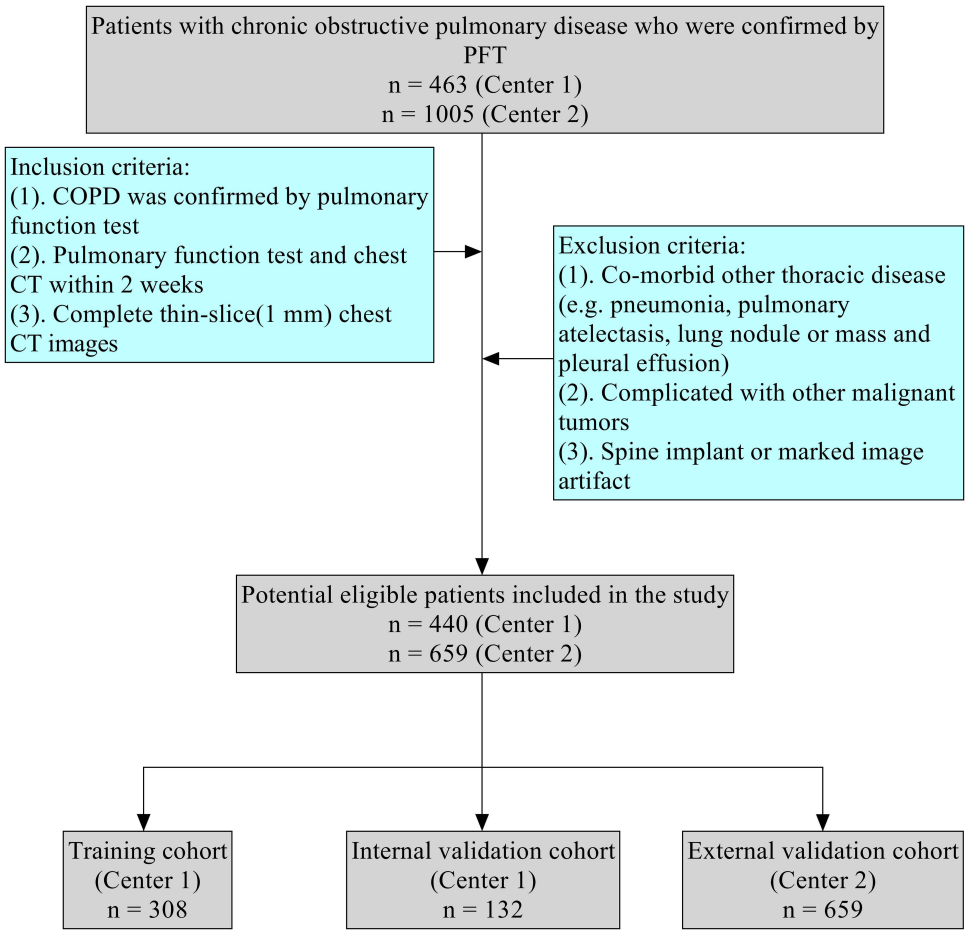

Figure 1 Flowchart showing patient screening.

was performed using CHEST Multifunction Spirometer HI-801 (Japan). The interval of Chest CT and PFT was within 2 weeks.

Whole-Lung Segmentation

The automatic segmentation based on our previous studies was utilized.[24–26] Briefly, a publicly accessed deep-learning model, U-net (R231) (https://github.com/JoHof/lungmask), was used to automatically segment the right lung and left lung. The same segmentation process and assessment method was used throughout the study.[25,26]

Extraction of Radiomics Features

Open-source software PyRadiomics (version 3.0.1, https://pyradiomics.readthedocs.io/en/latest/) was utilized for extracting radiomics features. Prior to feature collection, image preprocessing was carried out to correct diverse pixel spacings of CT image volumes from cases obtained from two centers. Standard image preprocessing was detailed in Supplementary material 3,[27–29] which is related to reducing image noise and ensuring result reliability. The Dice coefficient was calculated to analyze the consistency between manually delineated whole-lung regions and automatically delineated ones. The first-order, shape, and texture features were then collected and normalized using Z-score normalization.[30]

Radiomics Feature Screening and Model Establishment

Optimal radiomics features were selected using the following approach. First, redundant features whose correlation coefficient with other features is greater than 0.90 were removed. After highly reproducible and reliable features were determined, the remaining features from different hospitals were harmonized using the combat method. Harmonized features were subsequently applied to construct and validate the radiomic model. During training, feature engineering was conducted to select the most predictive features and exclude redundant ones. Second, irrelevant and redundant features were eliminated using the minimal Redundancy Maximal Relevance (mRMR) algorithm. Then, 10 cross-validations were conducted to adjust the penalty parameter, and the best feature with a non-zero coefficient was selected. Finally, the products of all chosen features with their corresponding coefficients were summed up to calculate the rad-score, based on LASSO logistic regression coefficients. Thereafter, the radiomics features-based logistic regression models were constructed. Radiomics feature selection and model establishment were carried out using a training set.

Risk factors with statistical significance were acquired using univariate logistic regression, which was then incorporated into multivariate regression for establishing the clinical and combined models. Last, a nomogram was constructed to visualize the combined model and graphically evaluate variable importance while calculating the prediction accuracy. Nomogram calibration was assessed by plotting calibration curves (Hosmer–Lemeshow test), while nomogram clinical practicability was assessed using a decision curve.

Statistical Analysis

Results were examined using R software (version 4.1.0 https://www.R-project.org). The classified data were analyzed using the chi-square test or Fisher's exact test, whereas continuous data were analyzed using the Mann–Whitney *U*-test and independent *t*-test for comparing baseline patient features. The ROC curve was analyzed to evaluate model prediction accuracy. AUCs among diverse models were compared using the DeLong test. P-values were normalized by the false-discovery rate for multiple comparisons. $p < 0.05$ was considered significantly significant.[31] The formulas for calculating Dice coefficient, accuracy, sensitivity, specificity, and AUC were provided in Supplementary material 4.

Results

Patient Characteristics and Construction of Clinical Model

Table 1 displays the clinical features of all the datasets. Among the 1099 patients with COPD (837 males, 262 females; age ranging from 25 to 93 years with an average age of 67.31 ± 9.83 years), 838 patients were mild-moderate COPD and 261 ones were severe/very severe COPD. The training set included 308 patients, including 233 in the GOLD I–II group and 75 in the GOLD III–IV group. The internal validation set included 132 patients, including 104 in the GOLD I–II group and 28 in the

Table 1 Patient Features of Three Datasets (Mean ± Standard Deviation)

Characteristics	Training Set (N = 308)			Internal Validation set (N = 132)			External Validation set (N = 659)		
	GOLD I–II (N = 233)	GOLD III–IV (N = 75)	p value	GOLD I–II (N = 104)	GOLD III–IV (N = 28)	p value	GOLD I–II (N = 501)	GOLD III–IV (N = 158)	p value
Age	67.4±9.6	69.7±9.6	0.075	65±10.3	68.7±8.9	0.084	70.18±0.5	70.39±0.7	0.827
Gender			0.025			0.001			<0.001
Male	182(78.1)	68(90.7)		82(78.8)	26(92.9)		340(67.9)	139(88.0)	
Female	51(21.9)	7(9.3)		22(21.2)	2(7.1)		161(32.1)	19(12.0)	
Height	162.5±7.6	165±6.3	0.010	163.5±8.1	163.6±8.1	0.967	163.2±0.4	167.1±0.6	<0.001
Weight	63.6±11.3	65±10.7	0.365	62.6±11.6	61.9±12.6	0.776	65.9±0.5	66.6±0.9	0.490
BMI	24±3.6	23.8±3.7	0.703	23.4±3.5	23±3.4	0.590	24.7±0.2	23.8±0.3	0.031
Smoking status			0.08			0.713			<0.001
Current Smoker	68(29.2)	18(24.0)		33(31.7)	11(39.3)		112(22.4)	53(33.5)	
Former Smoker	38(16.3)	21(28.0)		18(17.3)	5(17.9)		54(10.8)	28(17.7)	
Non-smoker	127(54.5)	36(48.0)		53(51.0)	12(42.9)		335(66.9)	77(48.7)	

GOLD III–IV group. 659 COPD patients from Center 2, including 501 in the GOLD I–II and 158 in the GOLD III–IV, were used as the independent external validation set. There was significant difference in gender between the GOLD I–II and GOLD III–IV groups in the training set and two validation sets ($p < 0.05$, Table 1). However, there were no significant differences in age and weight ($P > 0.05$). Height did not significantly differ between GOLD I–II and GOLD III–IV patients in the internal validation set. Besides, there were significant differences between two groups in variables of BMI and smoking status only in the external set ($P < 0.05$).

Univariable and multivariable analysis identified that age [odds ratio (OR) 1.04; 95% confidence interval (CI) 1.00–1.07; p = 0.025] and height (OR 1.06; 95% CI 1.02–1.10; p = 0.004) were independent predictors of the severity of COPD, and that these were also effective factors for clinical model construction. (Table 2)

Agreement Assessment Between Manual Segmentation and Fully Automatic Segmentation

Assessment of segmentation was performed using Dice index, an objective metric that quantifies the spatial overlap between two contours.[32] The mean Dice coefficient between the manual and automatic segmentation was 0.97 ± 0.06.

Feature Selection and Radiomics Signature Building

There were altogether 1,218 radiomics features obtained based on CT images from every COPD case. Of all the 1218 features, 100 features were original features, 430 features were processed applying Laplace of Gaussian filter and 688 features were processed applying Wavelet filter. More details about the extracted whole-lung radiomics features were in Supplementary material 5. At first, after Pearson's correlation analysis (absolute value of Pearson correlation coefficients

Table 2 Univariable and Multivariable Logistic Regression Analysis for Radiomics Nomogram

Characteristics	Univariate Regression		Multivariate Regression (Clinical Model)		Multivariate Regression (Radiomics Nomogram)	
	OR [95% CI]	P-value	OR [95% CI]	P-value	OR [95% CI]	P-value
Age	1.03 [1.00, 1.06]	0.08	1.04 [1.00, 1.07]	0.025	1.03 [0.99, 1.07]	0.107
Height	1.05 [1.01, 1.09]	0.01	1.06 [1.02, 1.10]	0.004	1.01 [0.96, 1.06]	0.691
Gender	0.37 [0.16, 0.85]	0.02	–	–	–	–
Radscore	3.32 [2.44, 4.51]	<0.001	–	–	3.32 [2.43, 4.54]	<0.001

> 0.9 were eliminated), a total of 241 stable radiomics features were retained. Second, irrelevant and redundant features were removed by mRMR, with 30 being preserved. Thereafter, LASSO was carried out for choosing the optimal feature subset for constructing the eventual model. Afterwards, optimal radiomics features with non-zero coefficients were selected by optimal λ obtained from LASSO regression via 10-fold cross-validation (Figure 2). At last, we chose thirteen radiomics features for constructing a radiomics signature. Radscore was calculated by the formula in Supplementary material 6.

Individualized Radiomics Nomogram Construction

Based on univariate regression analysis, Radscore ($P < 0.05$) was identified as another independent predictor of COPD severity. Multivariate regression was also carried out to develop the prediction model by integrating Radscore, age and height (Table 2).

Figure 3A shows the radiomics nomogram. The formula for calculating the nomoscore can be found in the Supplementary material 7. Calibration curves (Figure 3B–D) demonstrated that the nomogram exhibited good calibration across all three datasets. An example of application of the nomogram is shown in Figure 4.

Performances of Clinical Model, Radiomics Signature, and Nomogram

Table 3 displays the performance of the clinical model, radiomics signature, and nomogram in the diagnosis of training, internal, and external validation sets, respectively. Figure 5A–C display the ROC curves for the three models across the three datasets.

The AUC of the clinical model for identifying the severity of COPD of the training set was 0.624, while the AUC for radiomics signature was 0.857, and for the nomogram, it was 0.865. The AUCs for the three models of the internal validation set were 0.556, 0.850, and 0.851, respectively, and those of the external validation set were 0.642, 0.774, and 0.781, respectively. The AUC value of the training set increased in radiomics signature compared to that of the clinical model ($P < 0.001$) and in nomogram relative to the clinical model ($P < 0.001$). Besides, both the AUC values of radiomics signature and nomogram markedly increased relative to clinical model in the internal and external validation sets ($P < 0.001$). The differences of AUCs between radiomic nomogram and radiomics signature in training ($p = 0.08$), internal ($p = 0.97$) and external validation sets ($p = 0.25$) were not statistically significant.

Figure 5D displays DCA for the three models. According to our DCA results, when the threshold probability for one case was >5%, the use of radiomics nomogram for identifying mild-moderate from severe/very severe cases was more beneficial than clinical model.

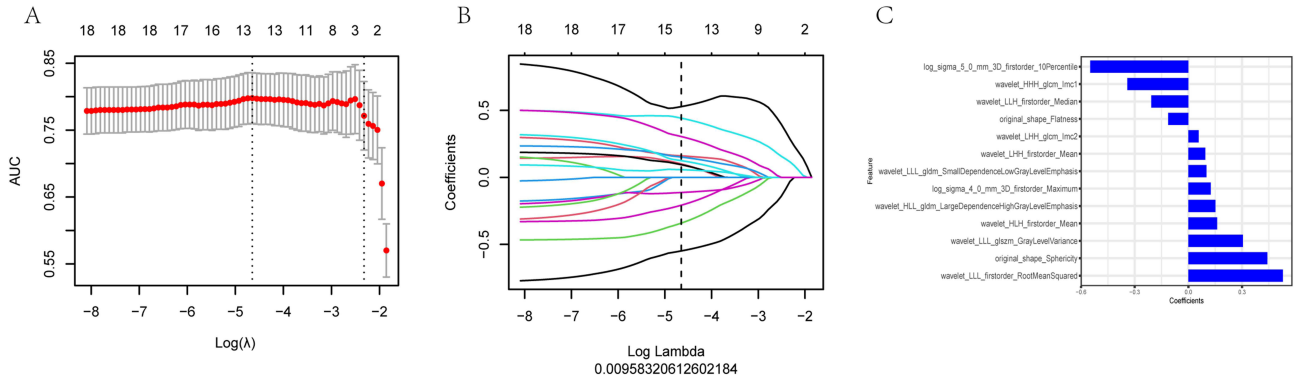

Figure 2 Optimal hyperparameter λ was chosen through LASSO regression by 10-fold cross-validation, and the lowest value indicated the feature best matched the real observations (**A**); Radiomics features of non-zero coefficients were identified by LASSO regression models (**B**); 11 radiomics features together with associated coefficients following dimensionality reduction via LASSO regression (**C**).

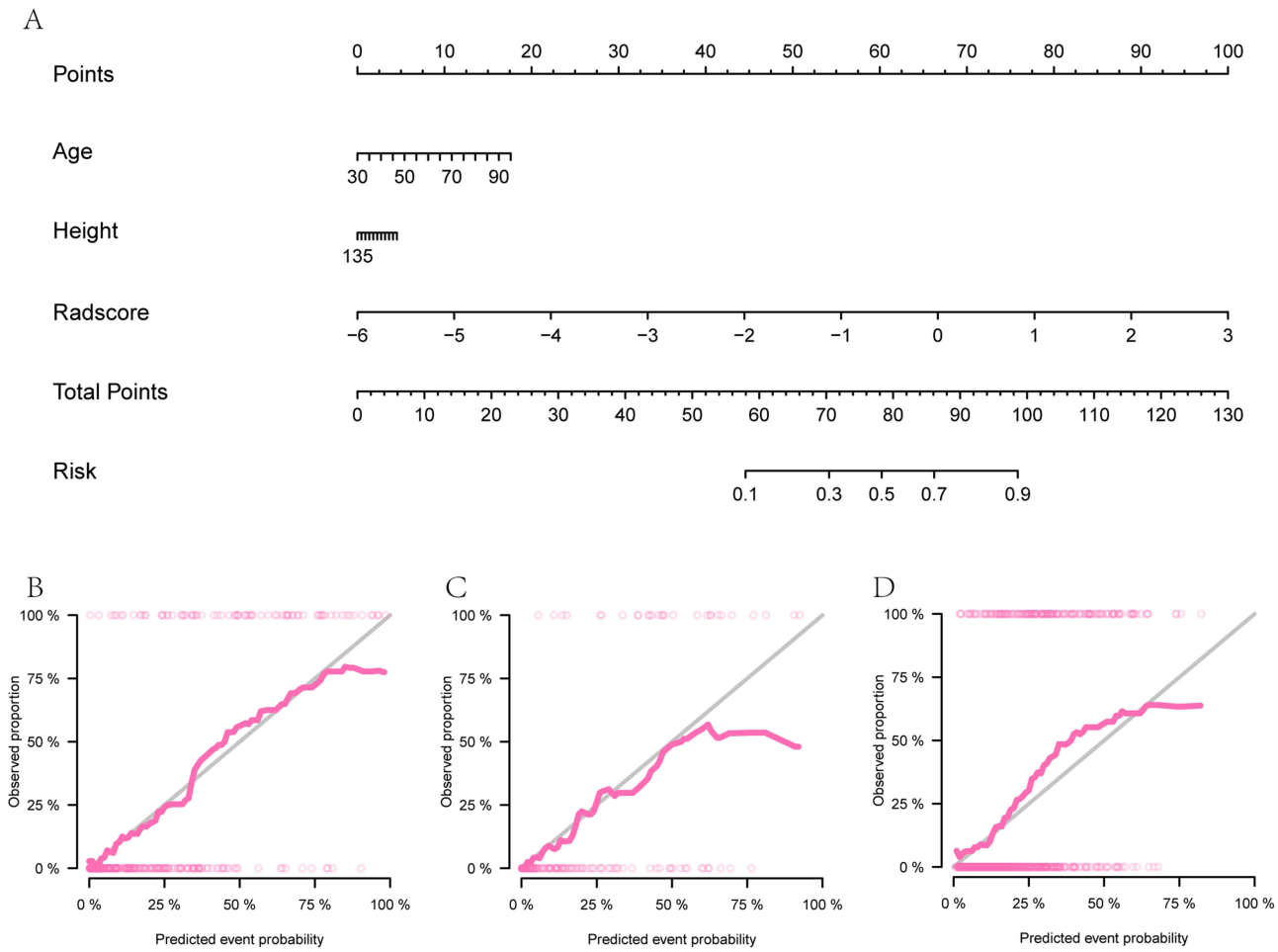

Figure 3 Radiomics nomogram constructed for predicting COPD severity (**A**); Calibration curve for the nomogram ((**B**–**D**) training, internal and external validation sets, separately).

Discussion

We constructed and validated the radiomics nomogram to identify the severity of COPD by the chest CT-based whole-lung radiomics signature incorporating age and height, showing the potential of clinical application feasibility. Moreover, radiomics signature could stratify the COPD severity independently, indicating the added value of chest CT to evaluate not only the pulmonary structure but also the lung function status.

The pretherapeutic assessment of COPD severity is of great importance, because it contributes to determining patient prognosis directly. It has been proven that the significantly higher complication rates in severe/extremely severe COPD patients were found in comparison with the mild-to-moderate COPD patients.[9] Therefore, early, rapid, economically feasible, and convenient diagnostic methods are in desperate demand. A series of studies have reported that CT morphological changes, such as bronchial wall thickening, trachea shape alterations as well as total lung emphysema percentage, are related to severe COPD patients. Pu et al[33] used lung function parameters to analyze emphysema together with airway wall thickening and found emphysema was closely related to FEV1/FVC (related to COPD diagnosis), and FEV1%predicted (associated with COPD severity).

Except for CT morphological research, several studies[21,34–36] suggest that CT-based radiomics can be used for quantifying COPD and uncovering the underlying disease mechanism. The radiomics signature is the easy decision-making support system. Lafata et al[34] analyzed the possibility of using CT images-extracted radiomics features for quantifying alterations of lung function and the underlying association with the spirometry test. Yang et al[21,35,36] used hybrid methods to combine deep learning and traditional machine learning approaches based on chest CT radiomics for

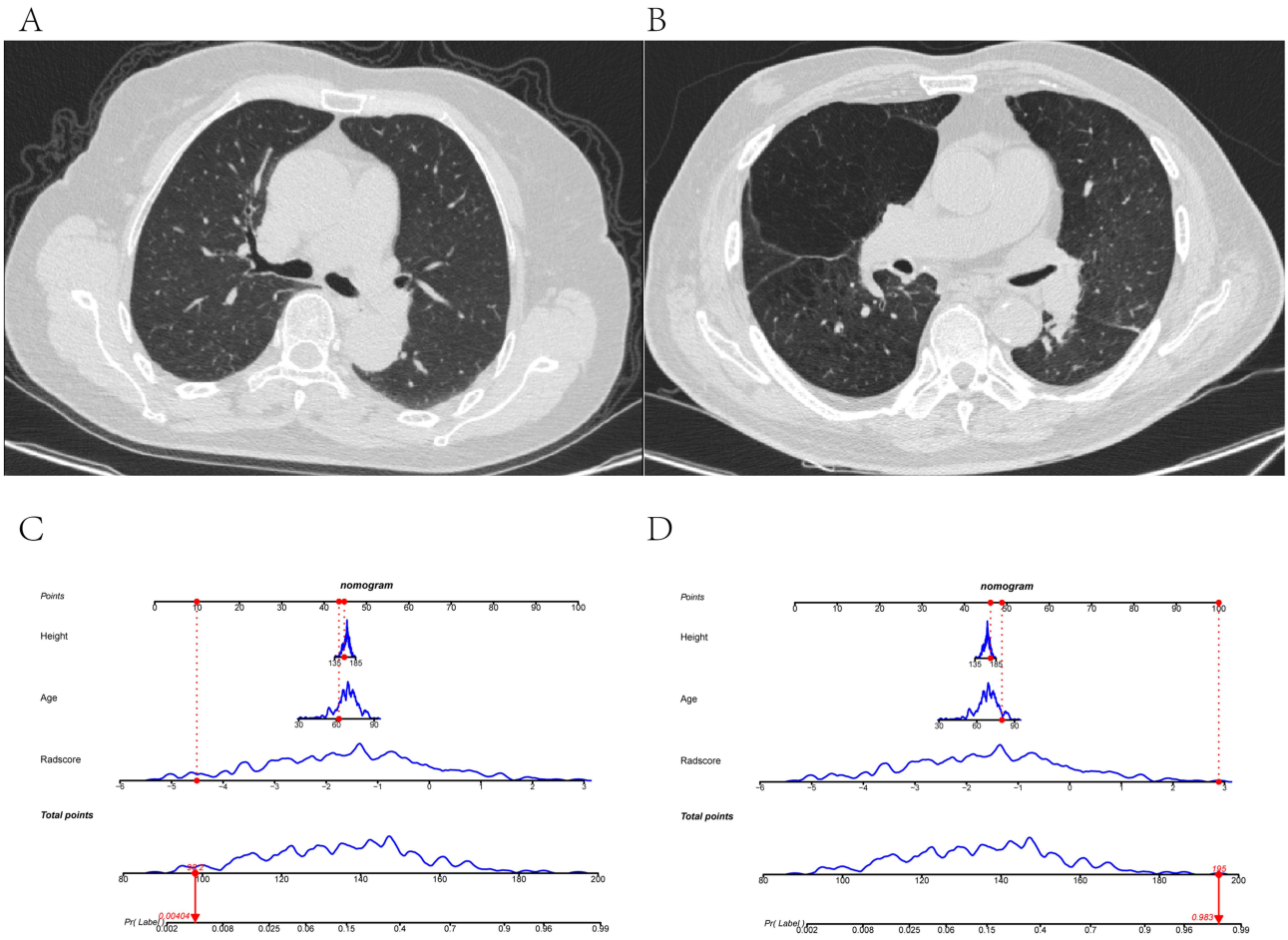

Figure 4 An example of the nomogram in clinical practice. (**A**) The nomogram was used to calculate the scoring process of risk of the severity of COPD. (**B**) Thin-section chest CT image of a 62-year-old female patient with mild-to-moderate COPD. Her clinical features were analyzed as follows: Height = 158 cm, Rad-score = −4.51. The nomogram showed that this patient had a total of 98.2 points after summing all points, which corresponds to a close to 0.4% probability of severe COPD. Pulmonary function test showed that the FEV1/FVC = 69.18%; FEV1% predicted = 93.7%. (**C**) The nomogram was used to calculate the scoring process of risk of the severity of COPD. (**D**) Thin-section chest CT image of an 80-year-old male patient with severe COPD. His clinical features were analyzed as follows: Height = 172 cm, Rad-score = 2.89. The nomogram showed that this patient had a total of 195 points after summing all points, which corresponds to a close to 98.3% probability of severe COPD. Pulmonary function test showed that the FEV1/FVC = 53.30%; FEV1% predicted = 37.5%.

identifying COPD cases and severity of COPD. All of the AUC values from these models were greater than 0.85, similar to ours in the training and internal validation sets. These studies emphasized on the algorithms and provided a good reference for us. To our best knowledge, there is a paucity of research applying whole-lung radiomics in COPD,[24–26] which could evaluate the heterogeneity of COPD comprehensively. Previous works focused on differentiating between COPD patients and non-COPD patients,[26] differentiating whether COPD patients have cardiovascular disease,[24] and differentiating between patients with preserved ratio impaired spirometry (PRISm) and COPD,[25] including those with FEV1/FVC ≥0.70 and FEV1 <80% predicted. These studies aim to identify patients with PRISm, a precursor condition to COPD, and comorbid COPD patients, in order to prevent or delay the onset of COPD through primary prevention measures and to improve the prognosis of COPD patients.

To enhance its applicability in routine clinical practice, we developed a nomogram utilizing whole-lung radiomics. This tool demonstrated commendable performance in differentiating the severity levels among patients with an established diagnosis of COPD. Such a methodology not only refines the categorization within the COPD cohort but also facilitates the formulation of tailored treatment plans and augments the prediction accuracy of patient outcomes. Among the 13 features most related to the severity, 9 wavelet features, 2 log-sigma features and 2 original features were identified. The wavelet features accounted for a large proportion. Wavelet features are a method based on wavelet transformation that can decompose images into sub-images with different scales and directions, thereby extracting local

Table 3 Diagnostic Performances of the Three Models in Three Sets

Model		Accuracy	Accuracy Lower	Accuracy Upper	Sensitivity	Specificity	AUC (95% CI)	p-value of DeLong-Test	
								vs Radiomics	vs Nomogram
Clinics	Training set	0.65	0.59	0.70	0.51	0.69	0.624 (0.552–0.696)	<0.001	<0.001
	Internal validation set	0.56	0.47	0.65	0.36	0.62	0.556 (0.432–0.681)	<0.001	<0.001
	External validation set	0.59	0.55	0.63	0.69	0.56	0.642 (0.596–0.688)	<0.001	<0.001
Radiomics	Training set	0.77	0.72	0.81	0.83	0.75	0.857 (0.808–0.906)	–	0.08
	Internal validation set	0.71	0.63	0.79	0.86	0.67	0.850 (0.779–0.921)	–	0.97
	External validation set	0.77	0.74	0.80	0.56	0.84	0.774 (0.731–0.817)	–	–
Nomogram	Training set	0.78	0.73	0.82	0.84	0.76	0.865 (0.818–0.913)	–	–
	Internal validation set	0.77	0.69	0.84	0.48	0.95	0.851 (0.778–0.923)	–	–
	External validation set	0.75	0.71	0.78	0.77	0.67	0.781 (0.740–0.823)	0.25	–

https://doi.org/10.2147/COPD.S483007

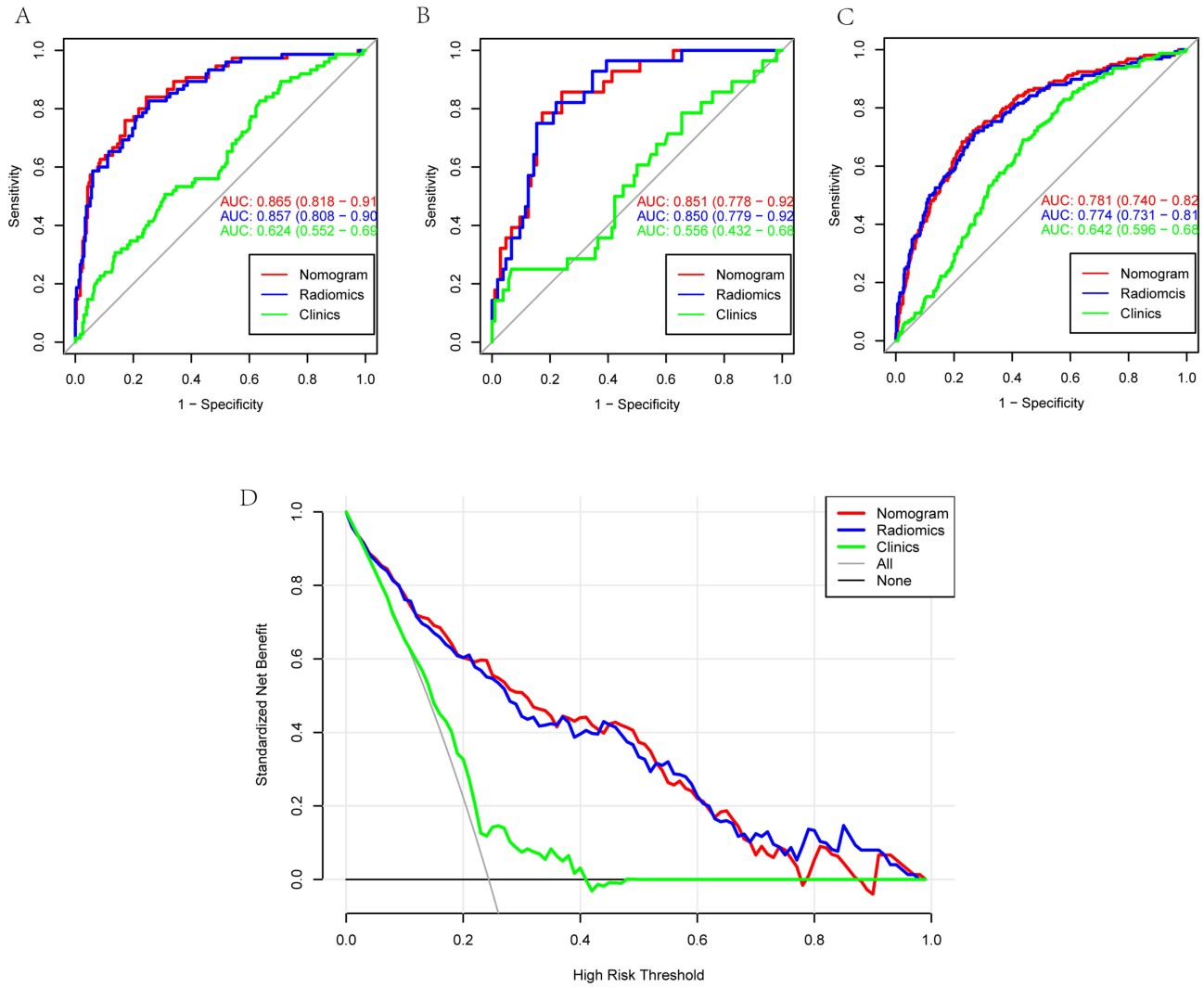

Figure 5 ROC curves for radiomics model, clinical model, and combined model in the prediction of COPD severity for training (**A**), internal (**B**) and external validation sets (**C**). DCA of clinical and combined models in the prediction of COPD severity (**D**).

features and patterns from the image. By analyzing the coefficients after wavelet transformation, texture, edges, structure, and shape information can be extracted from the image, providing a more abundant feature description for disease diagnosis and prediction. Previous studies have demonstrated the crucial role of radiomics in COPD.[18,21,22,37] Li et al[37] selected 42 non-overlapping ROIs at random in 11 axial CT sections in every patient and extracted radiomics features with the AUC of 0.799 and 0.797 based on SVM and LR, respectively, the performance is inferior to ours. Due to the diffuse characteristics, single or several ROI(s) of concern could not fully explain pulmonary changes. Therefore, the whole-lung radiomics analysis outperformed, just as our results with an AUC of 0.857, 0.850 and 0.774, in the training set and 2 validation sets, respectively. If clinical risk factors (such as age and height) were used in combination, the radiomics nomogram achieved a good discrimination effect, with AUCs of 0.865, 0.851, and 0.781 for training and validation sets, respectively. Although the radiomics nomogram showed a better performance than radiomics signature, no significant difference was found between it and radiomics signature (DeLong test, $p > 0.05$), indicating the value of radiomics signature for the severity assessment of COPD just based on the CT images independently, then adding the value of chest CT for both structure and function evaluation simultaneously.

Besides, clinical features like height and age independently predicted the risk of COPD severity. COPD severity is previously ascertained by the decrease of FEV1% predicted for age and height.[38] Our study showed age and height were also the predictive factors of COPD severity, which was consistent with the prior work.[39] Notably, radiomics nomogram has been frequently applied

in guiding the clinical decision-making in many diseases due to the easy to use in clinic. Recent reports and recommendations suggest that patients with severe COPD should be admitted for treatment.[40] Moreover, COPD is a chronic condition that needs long-time treatment to achieve persistent efficacy[41]; the quantitative radiomics nomogram can facilitate post-treatment follow-up alterations in COPD cases. Therefore, we built the nomogram incorporating the clinical and radiomics signatures. To assess the clinical practicability of radiomics nomogram, we also employed DCA, which sheds more light on clinical outcomes based on threshold probabilities, taking into account the net benefits (which were deemed to be true positive proportion minus false-positive proportion, weighted by relative harm of false-positive and false-negative results). DCA exhibited the increased overall net benefits of nomogram compared to that of the clinical model in predicting COPD severity among diverse threshold probabilities for diagnosing COPD. The nomogram can be used to distinguish the severe/very severe COPD from mild-moderate cases conveniently, guiding prompt treatment and improved prognosis. By enhancing the precision in assessing and categorizing COPD severity, healthcare providers can optimize treatment plans and forecast patient outcomes more accurately. This level of understanding facilitates exacerbation management, tailors therapeutic interventions, and ensures timely control of symptoms, potentially slowing disease progression.

Certain limitations must be noted in this work. First, pack-year smoking history were excluded due to greater than 50% missing values. Future investigations pay more attention to this variable. Second, the sample size of GOLD III–IV is small, although it is consistent with the epidemiological characteristics. Patients with different stages were not equally distributed, with relatively few cases of GOLD III–IV, thus probably skewing the results. Stratified sampling may reduce data bias. We will continue to collect more patients with GOLD III–IV and update the database in the future. Third, with the fast technological progresses of AI, the comparison between different AI models, including deep learning models, machine learnings, traditional CT features and CT quantitative parameters should be performed and compared in the future to understand the role of chest CT in the COPD evaluation comprehensively. Finally, due to the chronic nature of COPD, the relationship between COPD severity and prognosis with whole-lung radiomics was not investigated because of short follow-up. We will continue the follow-up of these cohorts.

Conclusion

In conclusion, this study constructed an easy-to-use radiomics nomogram for identifying the severity of COPD. By randomly selecting two patients and utilizing dynamic nomograms, we have illustrated the nomogram's potential clinical use. This model may function as a promising tool for guiding timely treatment and showing the added value of chest CT to evaluate the lung function status using only one-stop chest CT scanning besides the morphological assessment. Future research will focus on incorporating quantitative features, leveraging deep learning techniques, and employing multi-machine learning approaches to further optimize the model.

Abbreviations

COPD, Chronic Obstructive Pulmonary Disease; GOLD, Global Initiative For Chronic Obstructive Lung Disease; PFT, Pulmonary Function Test; FEV1/FVC, the ratio of forced expiratory volume in 1 second to forced vital capacity; FEV1%, predicted FEV1 percentage of predicted; CT, Computed Tomography; QCT, Quantitative Computed Tomography; ROI, Region Of Interest; BMI, Body Mass Index; NSCLC, Non-Small Cell Lung Cancer; GLCM, Gray Level Cooccurrence Matrix; GLSZM, Gray Level Size Zone Matrix; GLDM, Gray Level Dependence Matrix; mRMR, minimal Redundancy Maximal Relevance; LASSO, Least Absolute Shrinkage And Selection Operator; DCA, Decision Curves Analysis; AUC, Area Under The Curve; ROC, Receiver Operating Characteristic Curve.

Data Sharing Statement

The data will be available from the corresponding author on reasonable request.

Ethical Approval

This retrospective study using anonymized medical record data received an Institutional Review Board (IRB) waiver of informed consent from the Second Affiliated Hospital of Naval Medical University, as it involves no direct patient intervention and adheres to the Declaration of Helsinki. Patient privacy is fully protected, and ethical standards are strictly maintained.

Informed Consent

Written informed consent was waived by the Institutional Review Board.

Acknowledgments

We thank the colleagues in our department for their help in our study.

Author Contributions

All authors made a significant contribution to the work reported, whether that is in the conception, study design, execution, acquisition of data, analysis and interpretation, or in all these areas; took part in drafting, revising or critically reviewing the article; gave final approval of the version to be published; have agreed on the journal to which the article has been submitted; and agree to be accountable for all aspects of the work. The scientific guarantor of this publication is Li Fan.

Funding

This work was supported by the National Natural Science Foundation of China (82430065, 82171926, 81930049), the National Key Research and Development Program of China (2022YFC2010002, 2022YFC2010000 and 2022YFC2010005), the Medical Imaging Database Construction Program of National Health Commission (YXFSC2022JJSJ002).

Disclosure

The authors of this manuscript declare no relationships with any companies, whose products or services may be related to the subject matter of the article.

References

1. Deolmi M, Decarolis NM, Motta M, et al. Early origins of chronic obstructive pulmonary disease: prenatal and early life risk factors. *Int J Environ Res Public Health*. 2023;20:2294. doi:10.3390/ijerph20032294
2. Agustí A, Celli BR, Criner GJ, et al. Global initiative for chronic obstructive lung disease 2023 report: GOLD executive summary. *Arch Bronconeumol*. 2023;59:232–248. doi:10.1016/j.arbres.2023.02.009
3. Ruparel M, Quaife SL, Dickson JL, et al. Symptom burden, and underdiagnosis of chronic obstructive pulmonary disease in a lung cancer screening cohort. *Ann Am Thorac Soc*. 2020;17:869–878. doi:10.1513/AnnalsATS.201911-857OC
4. Goffin JR, Pond GR, Puksa S, et al. Chronic obstructive pulmonary disease prevalence and prediction in a high-risk lung cancer screening population. *BMC Pulm Med*. 2020;20:300. doi:10.1186/s12890-020-01344-y
5. Decramer M, Janssens W, Miravitlles M. Chronic obstructive pulmonary disease. *Lancet*. 2012;379:1341–1351. doi:10.1016/S0140-6736(11)60968-9
6. Hurst JR, Vestbo J, Anzueto A, et al. Susceptibility to exacerbation in chronic obstructive pulmonary disease. *N Engl J Med*. 2010;363:1128–1138. doi:10.1056/NEJMoa0909883
7. Jo YS. Long-term outcome of chronic obstructive pulmonary disease: a review. *Tuberc Respir Dis*. 2022;85:289–301. doi:10.4046/trd.2022.0074
8. Young KA, Strand M, Ragland MF. Pulmonary subtypes exhibit differential global initiative for chronic obstructive lung disease spirometry stage progression: the COPDGene® study. *Chronic Obstr Pulm Dis*. 2019;6:414–429. doi:10.15326/jcopdf.6.5.2019.0155
9. Cui F, Liu J, Shao W, He J. Thoracoscopic minimally invasive surgery for non-small cell lung cancer in patients with chronic obstructive pulmonary disease. *J Thorac Dis*. 2013;5(3):S260–266. doi:10.3978/j.issn.2072-1439.2013.08.25
10. Guo C, Yu T, Chang LY, et al. Mortality risk attributable to classification of chronic obstructive pulmonary disease and reduced lung function: a 21-year longitudinal cohort study. *Respir Med*. 2021;184:106471. doi:10.1016/j.rmed.2021.106471
11. Brown CD, Benditt JO, Sciurba FC, et al. Exercise testing in severe emphysema: association with quality of life and lung function. COPD. 2008;5:117–124.
12. Jones PW. Health status measurement in chronic obstructive pulmonary disease. *Thorax*. 2001;56:880–887. doi:10.1136/thorax.56.11.880
13. Park J, Hobbs BD, Crapo JD, et al. Subtyping COPD by using visual and quantitative CT imaging features. *Chest*. 2020;157:47–60. doi:10.1016/j.chest.2019.06.015
14. Han MK, Agusti A, Calverley PM, et al. Chronic obstructive pulmonary disease phenotypes: the future of COPD. *Am J Respir Crit Care Med*. 2010;182:598–604. doi:10.1164/rccm.200912-1843CC
15. Cho YH, Lee SM, Seo JB, et al. Quantitative assessment of pulmonary vascular alterations in chronic obstructive lung disease: associations with pulmonary function test and survival in the KOLD cohort. *Eur J Radiol*. 2018;108:276–282. doi:10.1016/j.ejrad.2018.09.013
16. Gallardo Estrella L, Pompe E, Kuhnigk JM, et al. Computed tomography quantification of tracheal abnormalities in COPD and their influence on airflow limitation. *Med Phys*. 2017;44:3594–3603.
17. Lee SM, Seo JB, Yun J, et al. Deep learning applications in chest radiography and computed tomography: current state of the art. *J Thorac Imaging*. 2019;34:75–85.

18. Yang F, Zhang J, Zhou L, et al. CT-based radiomics signatures can predict the tumor response of non-small cell lung cancer patients treated with first-line chemotherapy and targeted therapy. *Eur Radiol*. 2022;32:1538–1547. doi:10.1007/s00330-021-08277-y
19. Li Y, Xu Z, Lv X, et al. Radiomics analysis of lung CT for multidrug resistance prediction in active tuberculosis: a multicentre study. *Eur Radiol*. 2023;33:6308–6317. doi:10.1007/s00330-023-09589-x
20. Zhang Z, Wang Z, Yan M, et al. Radiomics and dosiomics signature from whole lung predicts radiation pneumonitis: a model development study with prospective external validation and decision-curve analysis. *Int J Radiat Oncol Biol Phys*. 2023;115:746–758. doi:10.1016/j.ijrobp.2022.08.047
21. Yang Y, Wang S, Zeng N, et al. Lung radiomics features selection for COPD stage classification based on auto-metric graph neural network. *Diagnostics*. 2022;12:2274. doi:10.3390/diagnostics12102274
22. Zhou T, Tu W, Dong P, et al. CT-based radiomic nomogram for the prediction of chronic obstructive pulmonary disease in patients with lung cancer. *Acad Radiol*. 2023;30:2894–2903. doi:10.1016/j.acra.2023.03.021
23. Huang W, Deng H, Li Z, et al. Baseline whole-lung CT features deriving from deep learning and radiomics: prediction of benign and malignant pulmonary ground-glass nodules. *Front Oncol*. 2023;13:1255007. doi:10.3389/fonc.2023.1255007
24. Lin X, Zhou T, Ni J, et al. CT-based whole lung radiomics nomogram: a tool for identifying the risk of cardiovascular disease in patients with chronic obstructive pulmonary disease. *Eur Radiol*. 2024;34:4852–4863. doi:10.1007/s00330-023-10502-9
25. Zhou T, Guan Y, Lin X, et al. A clinical-radiomics nomogram based on automated segmentation of chest CT to discriminate PRISm and COPD patients. *Eur J Radiol Open*. 2024;13:100580. doi:10.1016/j.ejro.2024.100580
26. Zhou TH, Zhou XX, Ni J, et al. CT whole lung radiomic nomogram: a potential biomarker for lung function evaluation and identification of COPD. *Mil Med Res*. 2024;11:14. doi:10.1186/s40779-024-00516-9
27. Hong JH, Jung JY, Jo A, et al. Development and validation of a radiomics model for differentiating bone Islands and osteoblastic bone metastases at abdominal CT. *Radiology*. 2021;299:626–632. doi:10.1148/radiol.2021203783
28. Shafiq-Ul-Hassan M, Zhang GG, Latifi K, et al. Intrinsic dependencies of CT radiomic features on voxel size and number of gray levels. *Med Phys*. 2017;44:1050–1062. doi:10.1002/mp.12123
29. Sun R, Limkin EJ, Vakalopoulou M, et al. A radiomics approach to assess tumour-infiltrating CD8 cells and response to anti-PD-1 or anti-PD-L1 immunotherapy: an imaging biomarker, retrospective multicohort study. *Lancet Oncol*. 2018;19:1180–1191. doi:10.1016/S1470-2045(18)30413-3
30. Haga A, Takahashi W, Aoki S, et al. Standardization of imaging features for radiomics analysis. *J Med Invest*. 2019;66:35–37. doi:10.2152/jmi.66.35
31. Chia CS, Wong LCK, Hennedige TP, et al. Prospective comparison of the performance of mri versus ct in the detection and evaluation of peritoneal surface malignancies. *Cancers*. 2022;14:3179. doi:10.3390/cancers14133179
32. Taha AA, Hanbury A. Metrics for evaluating 3D medical image segmentation: analysis, selection, and tool. *BMC Med Imaging*. 2015;15:29. doi:10.1186/s12880-015-0068-x
33. Pu Y, Zhou X, Zhang D, et al. Re-defining high risk COPD with parameter response mapping based on machine learning models. *Int J Chron Obstruct Pulmon Dis*. 2022;17:2471–2483. doi:10.2147/COPD.S369904
34. Lafata KJ, Zhou Z, Liu JG, Hong J, Kelsey CR, Yin FF. An exploratory radiomics approach to quantifying pulmonary function in CT images. *Sci Rep*. 2019;9:11509. doi:10.1038/s41598-019-48023-5
35. Yang Y, Li W, Guo Y, et al. Lung radiomics features for characterizing and classifying COPD stage based on feature combination strategy and multi-layer perceptron classifier. *Math Biosci Eng*. 2022;19:7826–7855. doi:10.3934/mbe.2022366
36. Yang Y, Chen Z, Li W, et al. Multi-modal data combination strategy based on chest HRCT images and PFT parameters for intelligent dyspnea identification in COPD. *Front Med*. 2022;9:980950. doi:10.3389/fmed.2022.980950
37. Li Z, Liu L, Zhang Z, et al. A novel CT-based radiomics features analysis for identification and severity staging of COPD. *Acad Radiol*. 2022;29:663–673. doi:10.1016/j.acra.2022.01.004
38. Pauwels RA, Buist AS, Calverley PM, Jenkins CR, Hurd SS. Global strategy for the diagnosis, management, and prevention of chronic obstructive pulmonary disease. NHLBI/WHO global initiative for chronic obstructive lung disease (GOLD) workshop summary. *Am J Respir Crit Care Med*. 2001;163:1256–1276. doi:10.1164/ajrccm.163.5.2101039
39. Thorington P, Rios M, Avila G, et al. Prevalence of chronic obstructive pulmonary disease among stable chronic disease subjects in primary care in Trinidad, West Indies. *J Thorac Dis*. 2011;3:177–182. doi:10.3978/j.issn.2072-1439.2011.03.03
40. Huang Q, Xiong H, Shuai T, et al. The clinical value of suPAR in diagnosis and prediction for patients with chronic obstructive pulmonary disease: a systematic review and meta-analysis. *Ther Adv Respir Dis*. 2020;14:1753466620938546. doi:10.1177/1753466620938546
41. Chen X, Tang S, Liu K, et al. Therapy in stable chronic obstructive pulmonary disease patients with pulmonary hypertension: a systematic review and meta-analysis. *J Thorac Dis*. 2015;7:309–319. doi:10.3978/j.issn.2072-1439.2015.02.08